

~~CONFIDENTIAL~~

Copy 6
RM E54L29



RESEARCH MEMORANDUM

PERFORMANCE OF A SUPERSONIC COMPRESSOR WITH SWEEP
AND TILTED DIFFUSER BLADES

By Arthur W. Goldstein and Ralph L. Schacht

Lewis Flight Propulsion Laboratory
Cleveland, Ohio

CLASSIFICATION CHANGED
UNCLASSIFIED

To _____

By authority of _____

NACA Re aded

YRN-123

Date

effective

Dec. 13, 1957

AMF 1-20-58

CLASSIFIED DOCUMENT

This material contains information affecting the National Defense of the United States within the meaning of the espionage laws, Title 18, U.S.C., Secs. 793 and 794, the transmission or revelation of which in any manner to an unauthorized person is prohibited by law.

NATIONAL ADVISORY COMMITTEE
FOR AERONAUTICS

WASHINGTON

March 28, 1955

~~CONFIDENTIAL~~

MAR 30 1955
LANGLEY AERONAUTICAL LABORATORY
LIBRARY, NACA
WALLLEY FIELD, VIRGINIA

NATIONAL ADVISORY COMMITTEE FOR AERONAUTICS

RESEARCH MEMORANDUMPERFORMANCE OF A SUPERSONIC COMPRESSOR WITH SWEPT AND
TILTED DIFFUSER BLADES

By Arthur W. Goldstein and Ralph L. Schacht

SUMMARY

A 14-inch supersonic mixed-flow compressor of large weight-flow capacity having a stator with swept and tilted blades was tested over a range of equivalent air tip speeds varying from 740 to 1700 feet per second. As rotor speed was increased over the entire range, stage efficiency decreased continuously from 73 to 47 percent and pressure ratio reached a value of 5.02. Large fluctuations in the pressure were found above an equivalent air tip speed of 1394 feet per second, at which speed a transition occurred from relative subsonic to relative supersonic velocities in the rotor. As the rotor speed was reduced toward design value for the stator, the normal flow configuration did not persist, as a consequence of the pressure of the fluctuations. For this reason low efficiency was obtained.

INTRODUCTION

To obtain compressors with high stage pressure ratio and large mass flow, considerable effort has been devoted to the development of compressors having supersonic velocities relative to the rotor. The major difficulty in the development of supersonic compressors for such high compression ratios is the large losses encountered in the stator. These losses reduce the adiabatic efficiency of the rotor-stator combination and therefore make the stage performance unattractive for practical application. Reference 1, for example, reports a reduction of rotor efficiency for the stage when a stator was added. Reference 2 reports a reduction of efficiency from 0.89 to 0.66 when stator blades were inserted downstream of the rotor. Reference 1 also shows that the diffuser prevented the rotor from operating at its optimum flow configuration.

The performance features of a series of supersonic rotors were investigated and reported in several papers (refs. 3 to 5). These rotors were all characterized by high turning (approximately 60°), inlet counter-rotation, and supersonic relative Mach numbers throughout at rotative

speeds near the design value. However, all showed the capability of operating in an alternative mode with strong shocks at the entrance and relative subsonic velocity internal to the rotor, but with an absolute supersonic discharge velocity having a subsonic axial component. Figure 1, which is the pressure-ratio and weight-flow diagram (data from ref. 4), shows a single point for supersonic internal flow and a curve of operation with strong inlet shock.

For rotors of this type, it is clear that the stator problem is severe. In the first place, the normal operating condition of the stator is at a high inlet Mach number - from 2.0 to 2.5, depending on the speed. (Normal mode of operation of rotor or stator is that state with designed wave system rather than the mode characterized by strong shocks at the entrance.) Secondly, the angle of attack will vary widely from the condition of normal operation of rotor to shock-in-rotor operation. Thus, not only must the diffuser start itself and operate effectively at high Mach numbers, but it must also permit the rotor to transit into normal operation at low supersonic Mach numbers and at high angles of attack corresponding to the presence of a strong shock at the rotor entrance. Separation of flow from the blade at large angles of attack can cause internal choking of the flow and provide effective internal flow areas less than the geometric area, thus preventing the starting of the rotor and stator.

The problem of operation at high Mach numbers has been approached by use of the principle of external compression as in the Oswatitsch diffuser. Researches (refs. 6 and 7) on the application of this principle to the design of supersonic rotors with subsonic axial velocity components indicate, however, that bow waves are set up with entrance normal shocks and that expected pressure recoveries are not attained. In addition to the application of the principle of external compression, the diffuser was designed with other features devised to facilitate the initiation of a normal flow configuration (without strong shocks) and to permit the attainment of a minimum Mach number before the terminating shock which reduces the velocity to a subsonic value. These include compression waves from the hub and case before entrance into the stator proper, the use of swept and tilted blades, and a terminating shock downstream of and exterior to the stator blades.

It did not prove possible, however, to provide sufficient internal stator contraction for efficient transition to subsonic velocities at the high incident Mach numbers and at the same time to maintain sufficient internal flow area to allow starting of the rotor from the condition of rotor-entrance shock and low supersonic discharge Mach number. Consequently, it appeared that the diffuser (stator) must be designed with a variable throat for operation as a compressor. However, for the purpose of investigating the novel design features of the stator blade configuration, it was decided to circumvent the mechanical difficulties

attending a variable throat by designing the stator for normal operation at 70 percent of the design speed of the original rotor (described in ref. 4) and to start the normal diffuser flow pattern by overspeeding to full rotor design speed (equivalent air tip speed of 1480 ft/sec) followed by a drop-off to the 70-percent value (equivalent air tip speed of 1036 ft/sec).

The present investigation was initiated at the NACA Lewis laboratory in order to determine the order of events in the process of starting the normal flow configuration, to determine whether the assumed limitations on starting are the actual limitations, and to determine whether a diffuser designed with the features of the present one could be efficient when operating at high Mach number and over a wide range of inlet angles.

DESIGN OF DIFFUSER

Basic Notions of the Design

General features of the diffuser design that were incorporated because of the high Mach number and the large variation of inflow Mach number and inflow direction are the following: In the first place, the span of the annular passage was decreased in passing from the rotor exit to the entrance of the stator blades (region AB, fig. 2). This not only decreases the Mach number for the flow striking the blades, but serves to decelerate the axial component at normal operating state and to accelerate this component when the rotor is operating with an entrance shock. Consequently, the angle variation between the two operating states is decreased. Secondly, the blade leading edges were swept back (fig. 2) to reduce the strength of a detached bow wave as well as that of the oblique shock present in normal operation. The sweep reduces the effective Mach number of blade operation by rendering irrelevant the velocity component parallel to the leading edge. Thirdly, the blade was tilted (i.e., rotated about a streamline on the suction surface) for two reasons: As the tilt of the stator blades increases, the shock wave attached to the leading edges will change orientation until it falls across the entrance or lip of the channel enclosed by the blades and walls. In the usual two-dimensional design with supersonic axial velocity, this orientation would have to be accomplished by increasing the blade wedge angle and the shock strength. Any internal normal shock that may arise in the process of establishing the normal mode of operation will therefore be weakened by the lip shock, and there will be a reduction in the losses. Also, this lip wave results in a decrease in the permissible minimum throat area and Mach number or in the approaching Mach number at which the normal wave configuration may be established.

As will be explained subsequently, the rotation or tilt of the blade also reduces the effect of variation of angle of attack of the inflow.

Inside the channel, the flow passage affords no further compression other than that which results from the wedge angle of the blade leading edge.

Consequently, as the blade is turned toward the axial direction, the blade span must be reduced. As the blade span is reduced in region BC, compression waves originate at the inner wall and are cancelled at the outer wall; whereas, in region CD the waves originate at the outer wall. The trailing edge is terminated on a characteristic surface. At location E an axially oriented shock provides the terminating compression for the diffuser. This location ensures an oblique terminating shock and also relieves the blade boundary layer of the necessity of sustaining the pressure rise accompanying the shock.

Unknown factors are necessarily involved in a radical design such as the present diffuser. In the first place, it is not known whether the procedure of designing for an average flow and then making corrections only for inflow angles is an adequate procedure. In the process of establishing the normal flow configuration, relief of the flow may possibly be encountered from unsteady or unsymmetrical flows and thus permit normal flow at lower than the estimated speed. A reverse effect may be expected if separation from the blades or walls causes an internal choke.

Some Design Details

In detail, the diffuser was designed for the average Mach number and inflow direction, and subsequently the blades of the stator were twisted for proper orientation in the field of flow, which varied from root to tip. The precontraction (region AB, fig. 2) was effected by a 4° semi-angle cone at the case (point A). This reduced the axial Mach number from 1.67 to 1.57 and the resultant Mach number from 2.02 to 1.93, with a flow-angle change from 34.1° to 35.6° . The maximum area reduction is limited, in that choking is avoided for any important compressor operating condition. Following the precompression, there was an outward deflection at the hub (point B) at the intersection of the first wave for a resultant turn of 15.2° . This resulted in reductions of the axial-radial component of the Mach vector from 1.57 to 1.07 and the resultant Mach number from 1.93 to 1.52, with a flow angle of 45.3° .

On the shock surface just defined (point BB, fig. 2), a meridional line served to define the leading edge of the blade, and the suction surface was a stream surface of the flow discharged from the shock surface. The pressure surface of the blade is taken as that for a minimum wedge angle (on the average about 8°) of the blade determined by structural and fabrication requirements.

For starting normal flow at the overspeed condition (equivalent tip speed, 1480 ft/sec), the rotor is assumed to be operating with entrance shock, and, when the gas flows into the expanded channel area between the stator blades, a normal shock results. If uniform one-dimensional flow is assumed, a contraction of the flow area to 0.89 of the inlet value would result in a choking flow. A contraction of 0.935 was incorporated into the design; and, consequently, the starting speed may be slightly lower than 1480 feet per second. Since the pressure-surface shock resulting from the blade wedge angle gives a slight overcompression, a slight internal expansion is required. Thereafter, a gradual turning of blade direction to 23° and a change of blade span were used to maintain the area constant and the Mach number at 1.4. The terminating shock exterior to the blades acted on the axial-velocity component alone, which was reduced from 1.29 to 0.78 of the local sonic velocity. The gas was discharged behind this terminating shock, with a resultant Mach number of 0.98 at an angle of 34° .

Effect of Tilt and Sweep

It will be recalled that the leading edge of the blade is on a meridional line located on the inclined shock surface. When the streamline at the hub passes back to the axial location of the blade-tip leading edge, there will be a considerable angular displacement, which results in a highly tilted blade. The tilt of the blades reduces the effective angle of attack for a given variation in flow angle, in that it places the blade surface more nearly in the surface containing the various inflow velocity vectors. A photograph of the rotor and stator is shown in figure 3.

The effect of sweep and tilt on angle of attack may be estimated according to the following: Assume a design flow vector directed along the unit vector \bar{t} , and assume that the off-design flow vector forms an angle α with respect to this in a plane having a normal unit vector \bar{k} (see fig. 4). Usually \bar{k} is directed along the leading edge. If such a blade surface including \bar{k} and \bar{t} is rotated around the vector \bar{t} by an angle σ , then σ is designated the angle of tilt. Cutting back the surface at an angle ϵ provides the sweep, so that the direction of the leading edge is given by unit vector

$$\bar{p} = (\bar{k} \cos \sigma + \bar{t} \times \bar{k} \sin \sigma) \cos \epsilon + \bar{t} \sin \epsilon$$

The effective angle of attack δ that results from the deviation of the vector \bar{V} from the design value \bar{V}_0 is

$$\tan \delta = \tan \alpha \frac{\cos \sigma}{\cos \epsilon - \sin \epsilon \sin \sigma \tan \alpha}$$

where $\bar{V}_0 \times \bar{t} = 0$ and $\bar{V} \times \bar{V}_0 = \bar{k} |V| |V_0| \sin \alpha$. Typical values of δ are as follows for $\sigma = 60^\circ$:

ϵ	0°	30°	60°	0°	30°	60°
α	$+30^\circ$	$+30^\circ$	$+30^\circ$	-30°	-30°	-30°
δ	16.1°	25.1°	76.9°	-16.1°	-14.5°	-17.2°

It is clear from the table that the effective flow-angle variation can be halved for $\sigma = 60^\circ$. Therefore, the efficiency of stator blades will probably be considerably improved over untilted blades for off-design operation. In the present case, the values were $\sigma = -25^\circ$ and $\epsilon = 18^\circ$. The value of σ is too small to offer a large reduction in α . However, the alinement on the shock surface allowed only one degree of freedom, and it was thought better to select this on the basis of the blade sweep.

TEST RIG, INSTRUMENTATION, AND PROCEDURE

The test-rig installation, which was the same as described in reference 2, is shown with measuring locations in figure 5. The working fluid was Freon-12, which was circulated in a closed system.

Inlet stagnation temperatures and pressures were measured in the surge tank. Four static-pressure taps in the inlet nozzle were used for determining the weight flow using the nozzle calibration from numerous previous surveys at station 1. At station 1, three claw probes were used with four pressure taps on the hub and four on the casing to check the nozzle calibration. Hot-wire anemometers were also used at two circumferential locations at station 1 to study qualitatively the nonsteady flow. These were 0.1 mil in diameter. At the exit, wires of 1.0 mil \times 0.1 inch proved to be too weak to sustain the buffeting, and no data of this type could be obtained.

Measurements of the stator-discharge flow were made at station 5, about 5.56 inches downstream of the stator blade trailing edges. Four static-pressure readings on the hub and four on the casing were linearly interpolated to determine the static pressure. The wall tap pressures were always determined with all instruments retracted from the stream, because the presence of the instruments interfered with the readings. For over-all performance, total pressure was obtained by two claws, two rakes of ten circumferentially displaced tubes, and two rakes of five radially displaced tubes, all in fixed locations at station 5. The claw probes were used to determine the angular orientation of the other instruments.

For surveys, traverses were made with two claws and two tangential total-pressure rakes across the passage in steps of 0.1 inch to within 0.076 inch of the hub and casing.

Four thermocouples were used in each of the elbows leaving the collector for taking the exit total temperature. These thermocouples were calibrated with temperature surveys made at station 5 in the early part of the tests.

Check measurements of the rotor-discharge flow were made by surveying the passage at station 3 with two claw probes. Station 3 is 0.8 inch upstream of the leading edge of the diffuser blade tip. Five circumferentially located static taps on the casing and two hub taps at station 3 were linearly interpolated for the static pressure.

Static-pressure taps were installed all along the impeller casing, the diffuser passage centerline on the hub and the case, and along the midspan streamline on the pressure and suction surface of one diffuser passage.

The most reasonable evaluations of the reliability of the pressure measurements are believed to be the comparisons of the weight flows computed from surveys of the exit and that from surveys at the inlet and the nozzle calibration. At station 5 weight flows were always high. At an equivalent air tip speed of 1702 feet per second, there was a discrepancy of 7.8 percent; while at all other survey points, the discrepancy was less than 3.5 percent. At station 3 agreement was very poor. Therefore, station 3 data could only be used qualitatively or for trends.

To study the starting problem of the diffuser and the nonsteady flow, catenary diaphragm pressure pickups were used in five circumferential locations on the case at station 3. Three additional pickups were located halfway through three blade passages, and one more was located near the discharge end of the channel. Two tube adapters for the static-pressure pickups were also made up, so that fluctuations of the total pressure could be studied.

The performance of the compressor was determined over a range of back pressure from open throttle to surge at ten wheel speeds from 50 to 115 percent of the design rotor speed (1480 ft/sec equivalent value in air). The rotor design tip speed was 686 feet per second in Freon-12. The inlet tank pressure was maintained at 10 to 15 inches of mercury absolute during all tests, and inlet temperatures varied from 60° to 115° F, depending on the load on the cooling system. Freon purity was maintained over 97 percent.

RESULTS AND DISCUSSION

Tests of the rotor alone showed that, below the transition speed of 1000 feet per second (68 percent of design value), the pressure ratio varied with weight flow at a fixed speed in a manner similar to low-pressure-ratio stages, the pressure ratio increasing to a maximum and then decreasing as the throttle was closed (see fig. 1). All operating states were characterized by a static-pressure distribution on the outer case that rose sharply at the rotor entrance, indicating strong compression waves there. As the rotor was operated at higher speeds, a different mode of operation was observed, in that the strong entrance compression waves were absent and the relative flow inside the rotor was supersonic. Because of the forward turning of the blade trailing edges, the impulse mode of operation was also characterized by a discontinuous rise in work output and pressure ratio; and, because of the absence of the initial shock, the efficiency rose discontinuously. It was impossible to operate the rotor at intermediate states with a shock inside the rotor downstream of the entrance; the shock was always either at the entrance or downstream of the rotor because of the increase in flow area throughout the impeller.

Over-All Compressor Performance

With the diffuser inserted, the over-all stage performance was quite different, as may be seen from the plot of pressure ratio and weight flow for fixed speeds (fig. 6(a)). Included on the plot for comparison are two curves for the rotor alone at speeds of 1036 and 1480 feet per second. Figures 6(b) and 7(a) show the specific enthalpy rise (specific work input) and the adiabatic efficiency, respectively. At and above 1390 feet per second (94 percent of rotor design speed), the pressure distribution on the case showed that the impeller operated without strong entrance shocks. However, there were some differences from the corresponding mode of operation with rotor alone that will be discussed in more detail in a later section. When the rotor was started in this normal impulse mode of operation, the speed was reduced with open throttle to reach the stator design point at 70 percent of design rotor speed. However, at the transition speed of 1390 feet per second, the rotor always reverted to operation with strong entrance shocks. Although fair agreement was obtained on the method for estimating the starting condition (estimated value somewhat less than 1480 ft/sec), it was impossible to operate at design conditions and check on efficiency and pressure distribution against the theoretical values. Large pressure fluctuations were experienced at speeds higher than critical, which provided flow fluctuations large enough to ensure the transition to shock-in-rotor operation at all conditions where subsequent reversion to normal operation was impossible because of the diffuser limitation.

3547
Zero range of weight flow was obtained at speeds higher than the transition speed because of the extremely violent surge obtained whenever the compression shocks were forced to the rotor entrance by means of throttle adjustment. At 50 and 60 percent of design speed (air equivalent tip speeds of 740 and 890 ft/sec), where operation with rotor alone showed transition to internal supersonic velocities impossible to attain, no limit on the lower value of weight flow was observed. The upper limit of weight flow is plotted in figure 7(b), along with the maximum value for rotor alone for comparison. At 80-percent speed (1180 ft/sec tip speed) and lower, the diffuser is apparently choking as estimated and preventing the attainment of full flow. At 90-percent speed (1330 ft/sec) and higher, it is clear that no limit is imposed by the diffuser, which therefore permits starting of normal rotor operation as soon as the diffuser throat is sufficiently supercritical to cause transition of the rotor operating state.

2-MO
When the rotor was operated alone, it was noticed that specific enthalpy rise increased discontinuously when transition to normal impulse mode of operation occurred. Figure 7(c) shows the specific enthalpy rise for rotor alone operating in both modes and the rise for the complete stage. The enthalpy rises correspond to delivery of gas from the rotor at subsonic velocity. Consequently, transition to normal operation never occurred for the complete stage. This interpretation is probably incomplete, in that high-intensity flow fluctuations are believed to have a large effect on the flow.

Flow Fluctuations

Pressure pickups indicated very large fluctuations downstream of the rotor. In figure 8 are shown the data for rms fluctuation intensity of the pressures at the case as well as that indicated by a short total-pressure probe projecting into the stream. With the throttle wide open, the pressure fluctuations rise strongly on increase of speed over the transition value, both upstream and downstream of the stator blades. The same pattern at a higher level is noted for the total-pressure probes. The large increase probably results from passage of compression and expansion waves into the rotor from behind. Some corroboration for this hypothesis is obtained from the case pressure distribution, which, near the exit, is intermediate between that for shock-in-rotor and for impulse operation - a condition impossible to obtain with rotor alone. Thus, the pressure distribution is believed to correspond to some fluctuation because of lack of stability for the observed average pressure distribution.

When the throttle is closed sufficiently to eliminate expansion downstream of the stator blades or to position a shock at the discharge end, fluctuations are reduced, because the resultant pressure will not

[REDACTED]

oscillate from subsonic to supersonic. This situation would explain the difference in intensity between the fluctuations observed upstream and downstream of the stator. No change in static pressure could be observed upstream of the stator as the position of the downstream shock was varied.

The mechanism of the fluctuations is believed to be as follows: Surveys between the rotor and stator indicate a very large deficiency in stagnation pressure and velocity near the hub. Although the data are not believed to be accurate enough for quantitative work, this trend is nevertheless unmistakable. Therefore, this portion of the gas would not sustain a strong shock (because of hub and blade deflections), which would move upstream through the low-velocity layers into the main body of the flow and into the rotor. However, under these circumstances, expansion waves would originate on the stator blade leading edges in the mainstream, overtake the shock waves, and eliminate them at some location in the rotor. The flow configuration would then be in the initial state and ready for a repetition of the process. Relative motion of the rotor and stator would cause the pressure waves to rotate. Below transition speed, choking of the stator would give rise to upstream shock and expansion waves, which, when interacting with the rotor, would give rise to a periodic pressure fluctuation.

The character of the pressure fluctuations was further analyzed by noting the intensity as a function of frequency. At each intensity peak the phase relation between the various pickups was used to find the rotative speed of the disturbance. The main results of this work are summarized in figure 9. At 90 percent of design rotor speed (fig. 9(a)), a peak is noted at rotor frequency, which indicates one or a group of channels operating differently from the rest. The observed total-pressure pickup shows, in addition, a peak at 2400 cps and at the blade frequency of 3840 cps. The observed total-pressure fluctuations are very large. However, the interpretation to be placed on this data is not known, since this involves a stationary probe in a flow fluctuating in magnitude and direction and requiring correction as well for shock losses taking place in front of the instrument. At 96.2 percent of rotor design speed (fig. 9(b)), a single disturbance rotating at 1.22 times rotor speed is noted, as well as a peak at the blade frequency of 4160 cps and other small peaks. The character of these peaks (rotative speed, number of disturbances) was not sufficiently defined to interpret. The large total-pressure fluctuation peak was also too unsteady and complex in form for analysis.

At 113 percent of rotor design speed (fig. 9(c)), the single pulse rotating at approximately impeller speed was observed, as well as the peak at the same frequency as the passage of the rotor blades. A disturbance frequency of 1086 cps dominated the frequency spectrum. From the available data, this could correspond to either 17 waves about the periphery rotating at 0.3 of rotor speed or to 5 waves rotating at exactly

the rotor speed. A harmonic series is to be noted at the frequencies of 220, 440, 880, 1100, 1320, and 2200 cps, which are in the ratio of 1, 2, 4, 5, 6, and 10, with the 220 and 440 cps disturbances corresponding to a single and double wave rotating at rotor speed. Therefore, it appears that the rotor frequency approached resonance with some natural frequency of the system in the neighborhood of 1100 cps.

Thus, the unsteady operation appears to arise from periodic motion of strong waves originating in and feeding backwards through the low-velocity gas near the blade roots and moving into the rotor through the mainstream, followed by expansion waves in the mainstream. These fluctuations are reinforced when their frequency coincides with that of a harmonic of an ever-present disturbance resulting from nonuniform operation of the various rotor channels. Clearly, if the flow cannot be stabilized, it is impossible to utilize the variable-throat diffuser, because the normal wave pattern will not return once it is disturbed and the throat of the stator is constricted.

Static-Pressure Distribution

The operating state of the rotor may be determined from the pressure distribution on the case, as shown in figure 10. At 70 and 90 percent of rotor design speed (100 and 126 percent of stator design speed) a strong pressure rise near the entrance indicates internal subsonic flows at wide-open throttle. For comparison (fig. 10(a)), the pressure distribution for the rotor alone is shown where the internal flow is supersonic. Supersonic internal velocities are attained at full speed and 115 percent of full speed, as the pressure distributions show on comparison with the pressure distributions for the rotors alone for the normal and subsonic modes of operation (fig. 10(b)).

Several noteworthy deviations of the pressure distribution in the rotor of the complete stage from the distribution for the rotor alone may be observed at rotor design speed. Starting at $z = 6$ inches, there is an increasing pressure increment that was not obtainable with the rotor alone. In the rotor tests, either the high-level or the low-level pressure distribution could be obtained, but nothing intermediate. At $z = 9.5$ inches, there is a further sharp rise in the pressure level, which may be ascribed to the inward deflection of 4° of the case. Because the deviation inside the rotor was not obtainable with steady-state operation of the rotor alone, it is reasonable to suppose that this discrepancy results from fluctuation of the pressure. As remarked previously, these fluctuations probably originate from penetration of alternate compression and expansion waves into the rotor from behind.

Figure 11 shows the static-pressure distribution on the outer and inner walls of the stators at open throttle for 90 and 100 percent of

3547

back
CV-2-10

design rotor speed. Calculations using the total pressures measured at diffuser exit (station 5) and the static pressures along the diffuser show that the velocities are supersonic at speeds of 94 percent of design rotor speed and higher. Because the assumed total pressure is low if in error, the estimated Mach numbers are also low if in error. Consequently, a strong stable shock wave cannot be assumed at the entrance to the channels between the stator blades. The most likely situation is a shock in front of the stator oscillating into the rotor, decreasing the rotor work input to the gas by reducing the through-flow velocity from the blades which were turned forward (see fig. 7(c)). The presence of this wave prevented the stator from ever attaining a normal supersonic internal flow configuration. The continuous character of the efficiency curve (fig. 7(a)) also confirms this notion. A jump in efficiency should have occurred at the transition speed of 94 percent of design, because a discontinuous jump in rotor efficiency is expected there and the losses attributable to the stator are roughly constant at 5 percent of the work input. However, the expected rise in efficiency is not evident; and, consequently, the change in rotor operation to supersonic discharge did not occur.

The various data which confirm this description of the flow are as follows: First, the pressure distribution on the case indicates a normal wave configuration in the front part of the rotor and an unstable configuration in the rear part. Second, the work output indicates low discharge velocities. Third, the variation of efficiency indicates the presence of strong, inefficient shocks in the rotor. Finally, large pressure fluctuations were measured downstream of the rotor.

Summary of Results

The high-solidity supersonic compressor was found to have the following characteristics:

1. For operation at open throttle, a transition in the mode of operation of the rotor occurred as the speed was increased to values higher than 94 percent of design (equivalent airspeed, 1390 ft/sec). This is in reasonable agreement with the estimation of somewhat less than 1480 feet per second. The high-speed mode was characterized by supersonic internal flow, whereas the low-speed mode exhibited a strong shock at the entrance and subsonic internal velocities. After transition, the compressor was operable at only one weight flow because of a surge limitation. At low speeds a wide range of weight flow with stable operation was obtained.

2. The over-all efficiency of the compressor was low (fig. 7(a)), decreasing continuously from 73 percent at 50-percent speed to 47 percent at 110-percent design rotor speed (equivalent airspeeds, 740 and 1630 ft/sec, respectively). Pressure ratios of 3.5 and 5.0 were obtained at

tip speeds of 1480 and 1702 feet per second, respectively (fig. 6(a)). At 90-percent speed and higher, maximum weight flow was not limited by the diffuser and was 64 pounds of Freon-12 per second.

3. A high level of pressure fluctuation was found after the transition speed was reached. When the speed was reduced, these fluctuations inhibited stabilization of diffuser and rotor operation with normal supersonic flow configurations, thus preventing attainment of the stator design condition at a rotative speed of 1040 feet per second. Fluctuation intensity increased with resonance between the rotor and stator. Unless these fluctuations can be eliminated, the variable-throat diffuser cannot be applied in compressors of this type.

4. After transition had occurred, pressure distributions were measured on the rotor casing which were unobtainable with steady-state operation of the rotor alone and which, therefore, indicate an unstable situation. It is reasonable to suppose that pressure fluctuations were present when such pressure distribution was measured.

5. Although the internal flow in the stator is supercritical above the speed for transition in the mode of rotor operation, it is believed that an unstable shock occurs in the region upstream of the stator and in the rear portion of the rotor. As a consequence, the work output of the rotor never exhibits the large values found in tests of the rotor alone, and the stage efficiency does not exhibit the expected jump in passing from subcritical to supercritical rotor speeds.

CONCLUDING REMARKS

When the rotor was being designed, the extent of the difficulties of the problem of initiation of normal flow in the compressor was not appreciated. In particular, if the rotor-diffuser combination had been designed for efficient operation at a speed for which it was possible to initiate the normal flow configuration, a substantial increase in efficiency would be expected. The present rotor cannot satisfy this requirement for any diffuser. A more satisfactory one would deliver gas, when operating normally, at a very different flow angle than when operating with internal shock. This would, of course, impose a severe condition on the stator. A special wide-range stator would be required, such as one with tilted or slotted blades.

Several methods are available to stabilize operation of the stage. First, because it is believed that the fluctuations arise in the boundary layer on the hub and case, removal of this low-energy gas would probably be helpful. Second, because fluctuation intensity increased with resonance between the rotor and stator, decoupling these would be helpful. This could be accomplished by using rotor-discharge annular areas giving more

██████████

nearly critical flows that could support only weak waves, and by discharging more nearly critical flows relative to the rotor.

Lewis Flight Propulsion Laboratory
National Advisory Committee for Aeronautics
Cleveland, Ohio, December 21, 1954

██████████

APPENDIX - SYMBOLS

The following symbols are used in this report:

- ΔH increase in specific stagnation enthalpy from station 0 to station 5, Btu/lb
- ΔH_{1s} increase in specific enthalpy at constant entropy from $P_{T,0}$ to $P_{T,5}$, Btu/lb
- \bar{k} unit vector normal to plane containing velocity vectors
- P static pressure, lb/sq in.
- P_T absolute stagnation pressure, lb/sq in.
- \bar{p} unit vector along leading edge
- \bar{t} unit vector along normal flow component
- z axial distance measured from leading edge of impeller blade root, in.
- α angle of attack, angle between normal and off-design flow vectors
- δ effective angle of attack
- ϵ sweep angle, angle of rotation about vector $\bar{t} \times \bar{k}$
- η_{ad} adiabatic efficiency of rotor, $\Delta H_{1s}/\Delta H$
- σ angle of tilt, angle of rotation of blade about vector \bar{t}

Subscripts:

- c casing
- e equivalent values for standard pressure and temperature
- 0 entrance tank upstream of nozzle (fig. 5)
- 1 station at rotor entrance (fig. 5)
- 3 station about 0.8 in. upstream of diffuser leading edge at tip (fig. 5)
- 5 station about 5.56 in. downstream of diffuser tip trailing edge (fig. 5)

REFERENCES

1. Jacklitch, John J., Jr., and Hartmann, Melvin J.: Investigation of 16-Inch Impulse-Type Supersonic Compressor Rotor with Turning Past Axial Direction. NACA RM E53D13, 1953.
2. Hartmann, Melvin J., and Tysl, Edward R.: Investigation of a Supersonic-Compressor Rotor with Turning to Axial Direction. II - Rotor Component Off-Design and Stage Performance. NACA RM E53L24, 1954.
3. Goldstein, Arthur W., and Schacht, Ralph L.: Performance of a Swept Leading Edge Rotor of the Supersonic Type with Mixed Flow. NACA RM E52K03, 1953.
4. Goldstein, Arthur W., and Schacht, Ralph L.: Performance of a Supersonic Mixed-Flow Rotor with a Swept Leading Edge and 0.52 Inlet Radius Ratio. NACA RM E53H27, 1953.
5. Schacht, Ralph L., Goldstein, Arthur W., and Neumann, Harvey E.: Performance of a Supersonic Rotor Having High Mass Flow. NACA RM E54D22, 1954.
6. Creagh, John W. R., and Klapproth, John F.: Utilization of External-Compression Diffusion Principle in Design of Shock-in-Rotor Supersonic Compressor Blading. NACA RM E53F18, 1953.
7. Jahnsen, Lawrence J., and Hartmann, Melvin J.: Investigation of Supersonic-Compressor Rotors Designed with External Compression. NACA RM E54G27a, 1954.

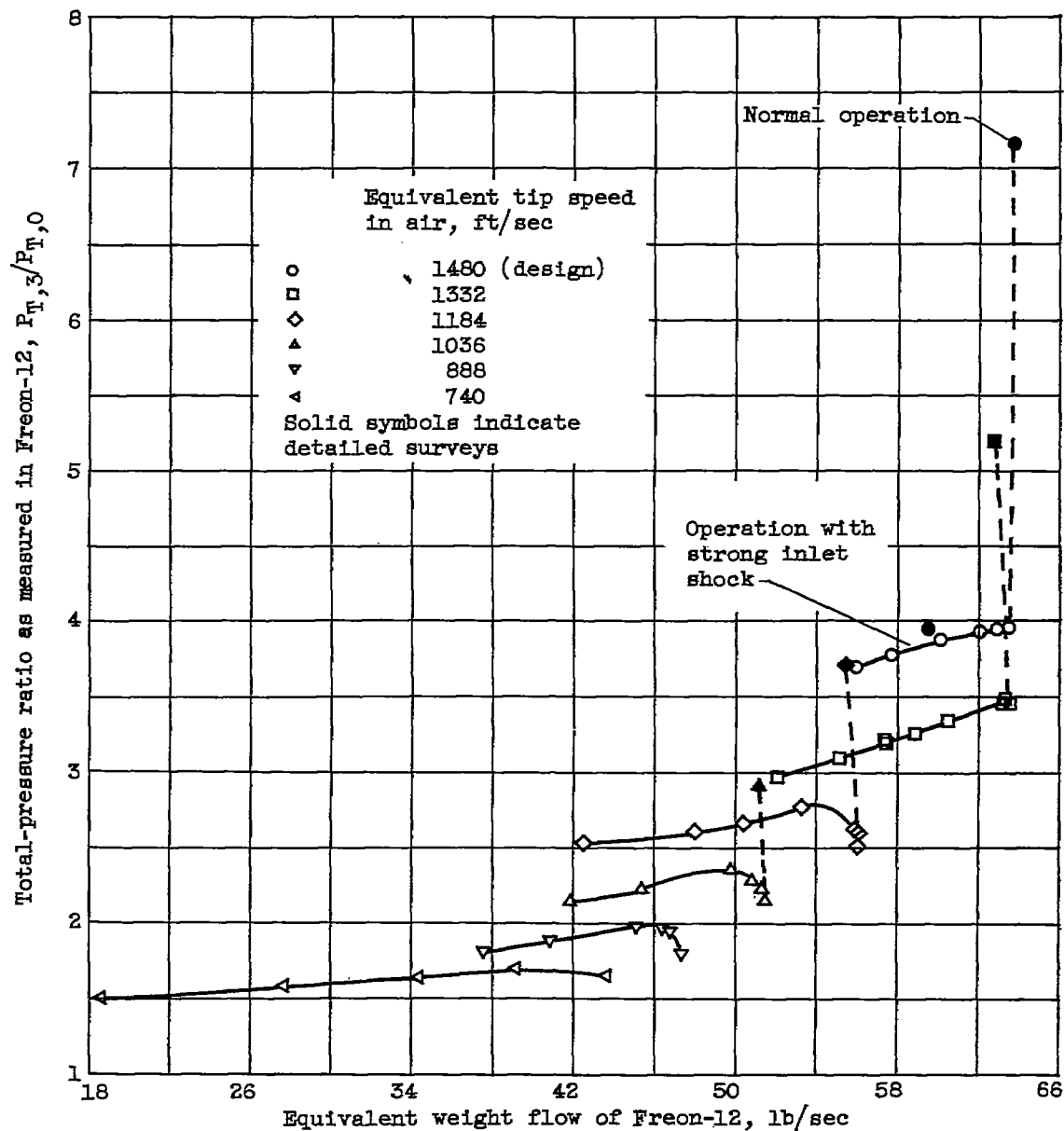


Figure 1. - Performance characteristics for 14-inch supersonic compressor rotor with 0.52 inlet radius ratio (ref. 4).

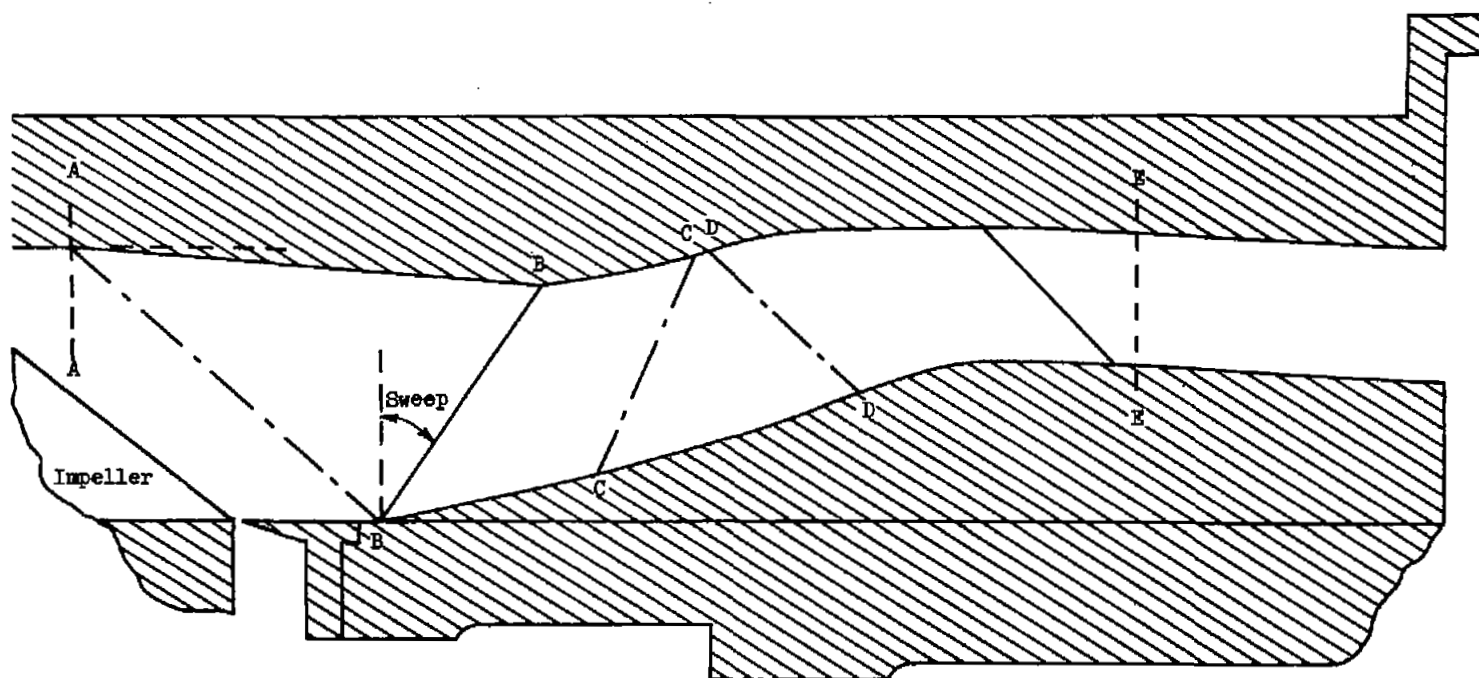
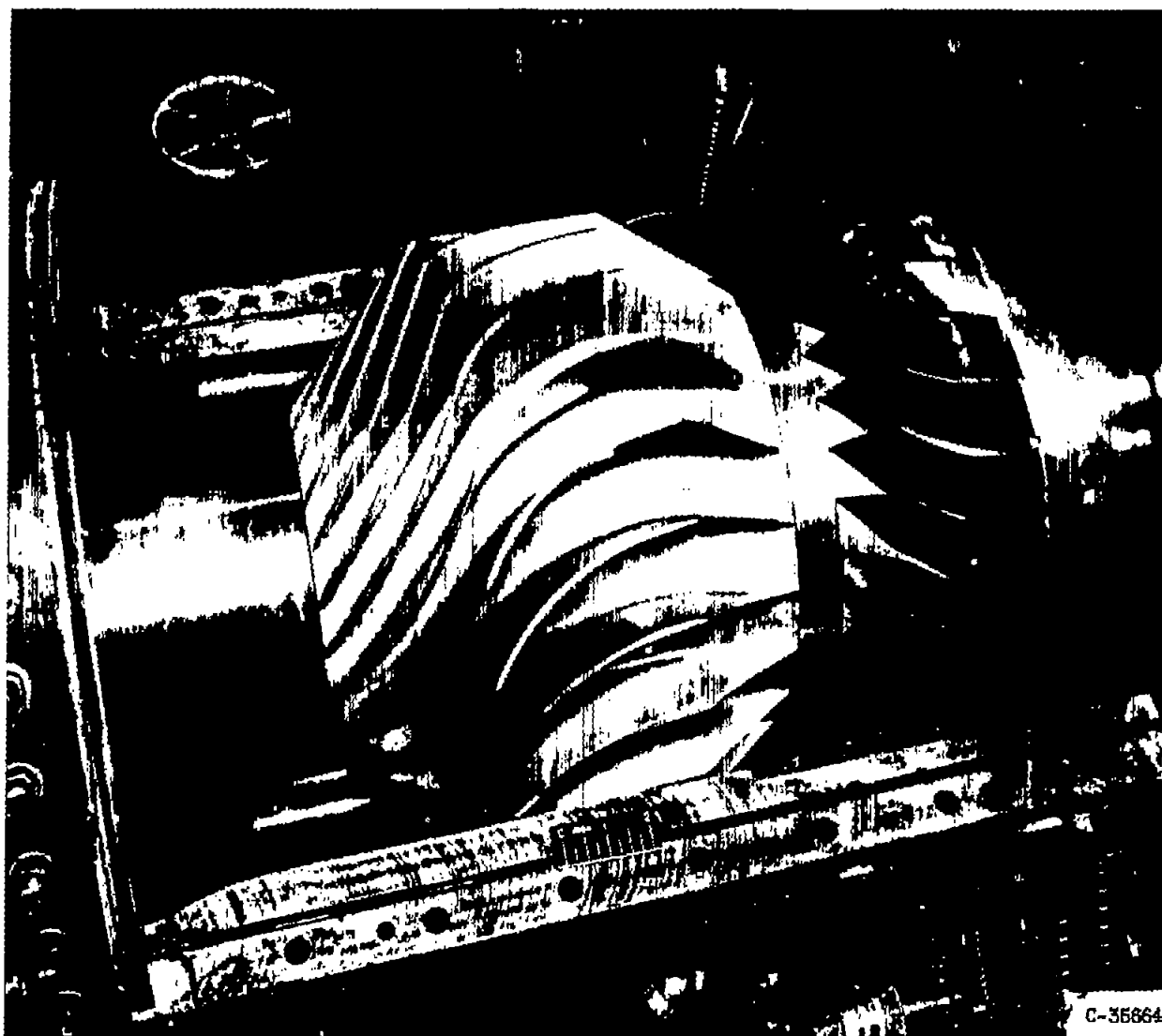
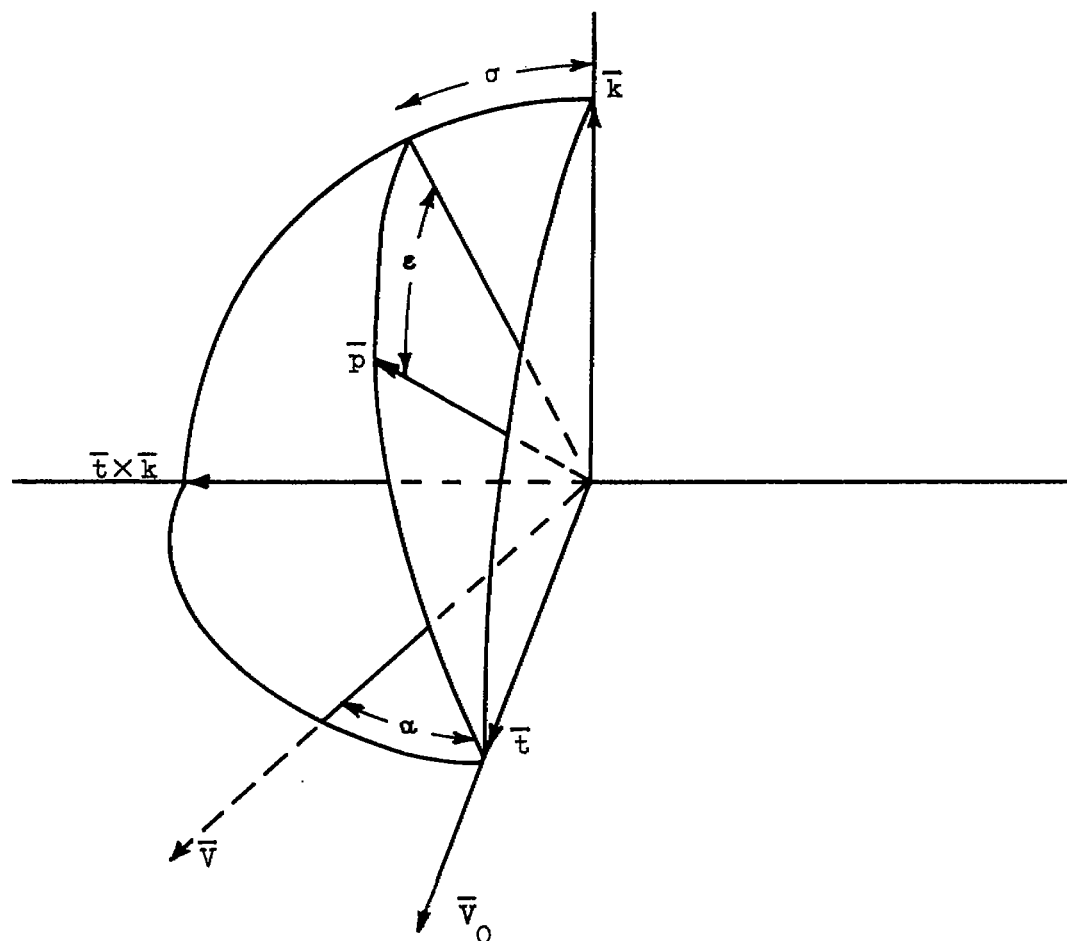


Figure 2. - Side-view diagram of diffuser.



C-35664

Figure 3. - 14-Inch supersonic compressor.



ϵ Sweep
 σ Tilt
 α Angle of attack

Figure 4. - Sketch showing angle of attack, tilt, and sweep.

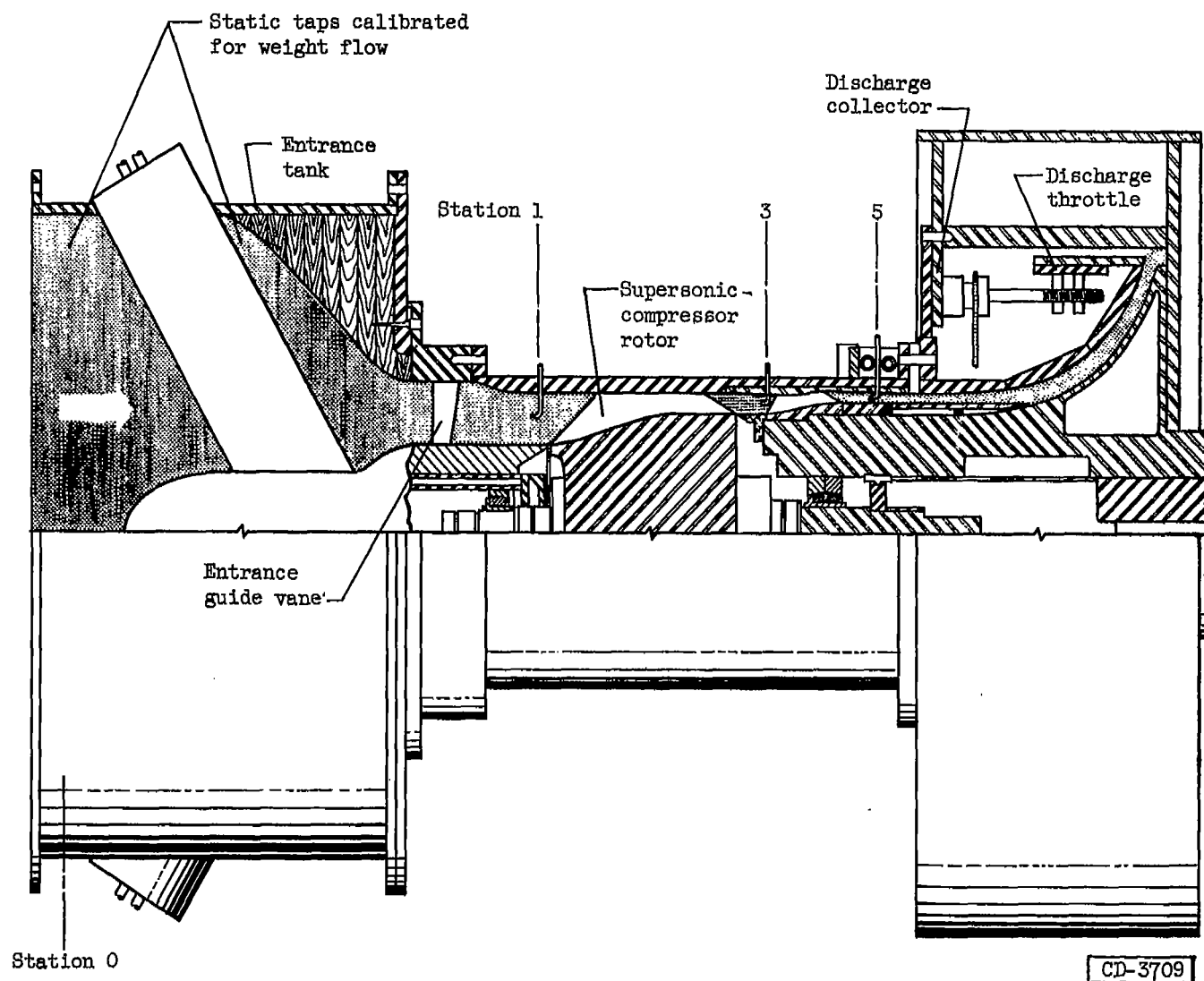
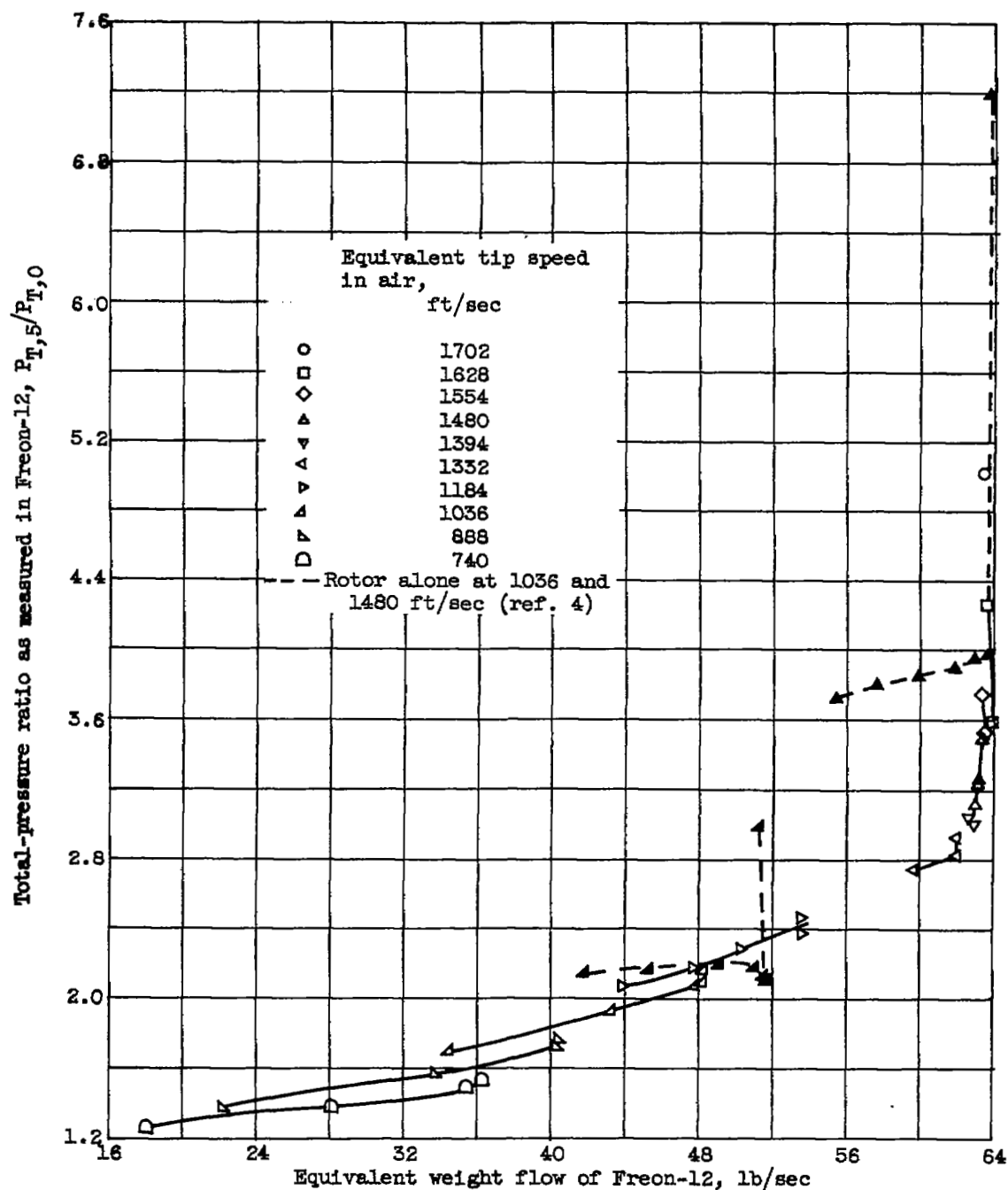
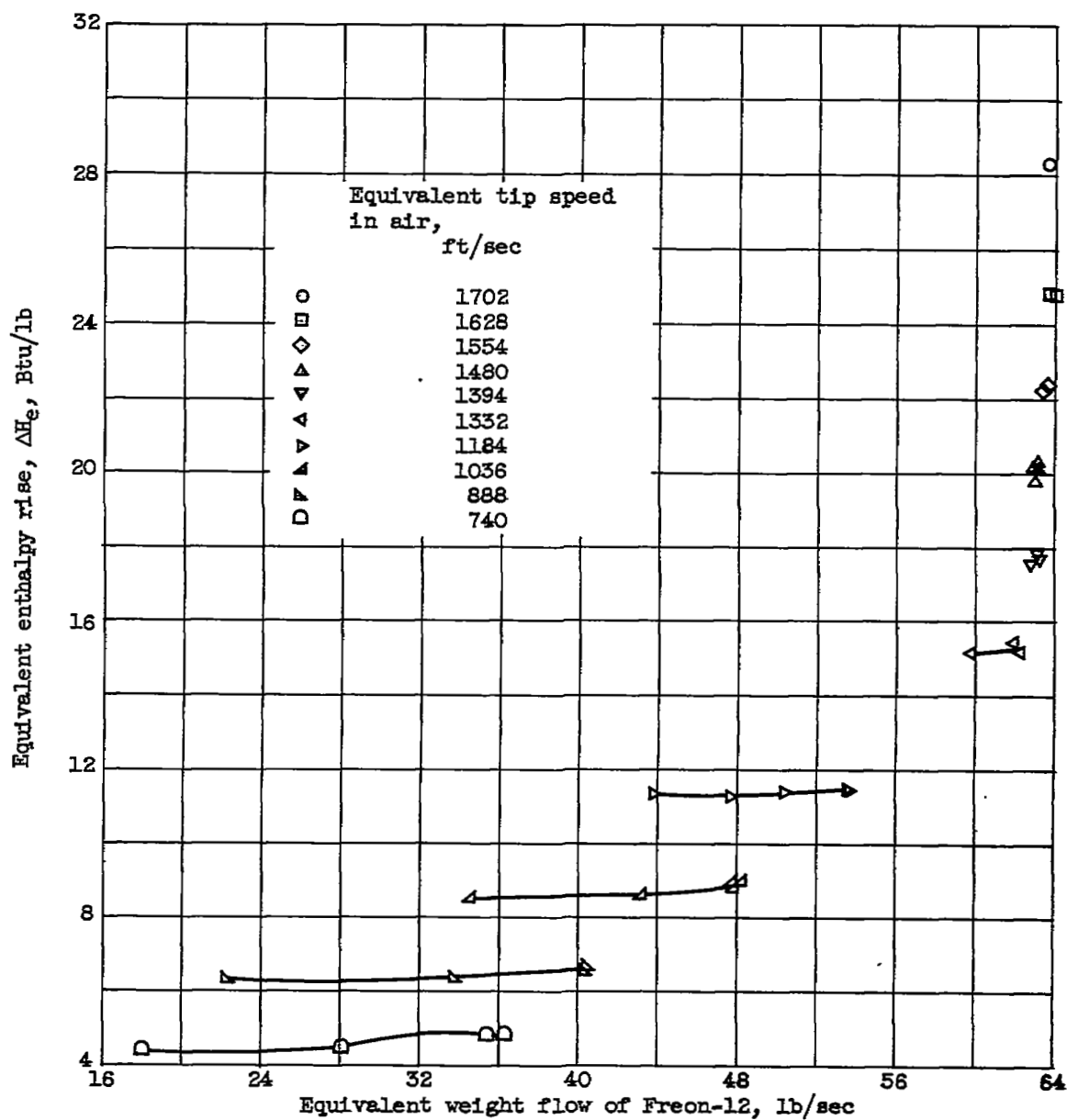


Figure 5. - Schematic diagram of 14-inch supersonic-compressor test rig.



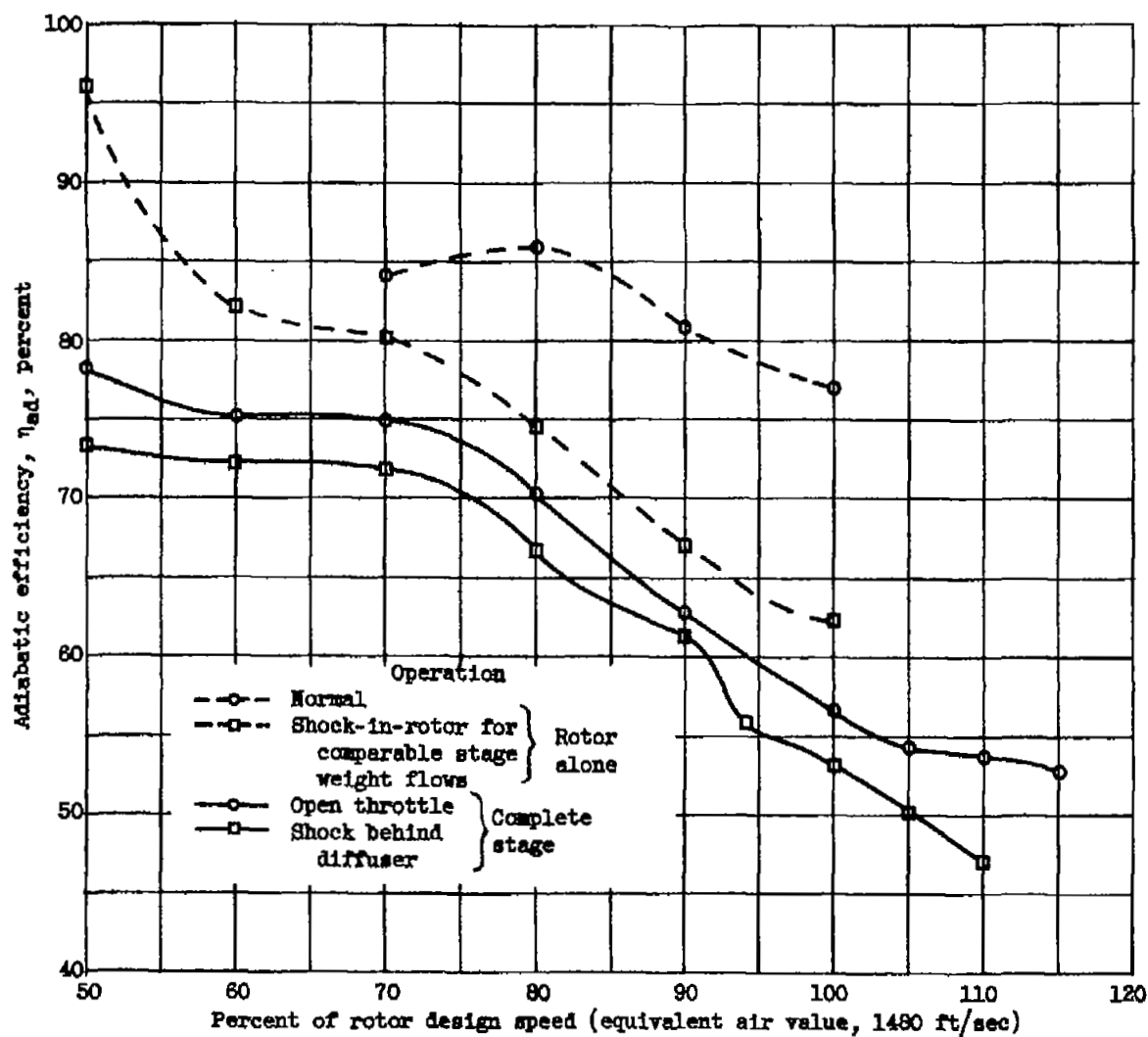
(a) Total-pressure ratio and weight flow.

Figure 6. - Performance characteristics for 14-inch supersonic compressor.



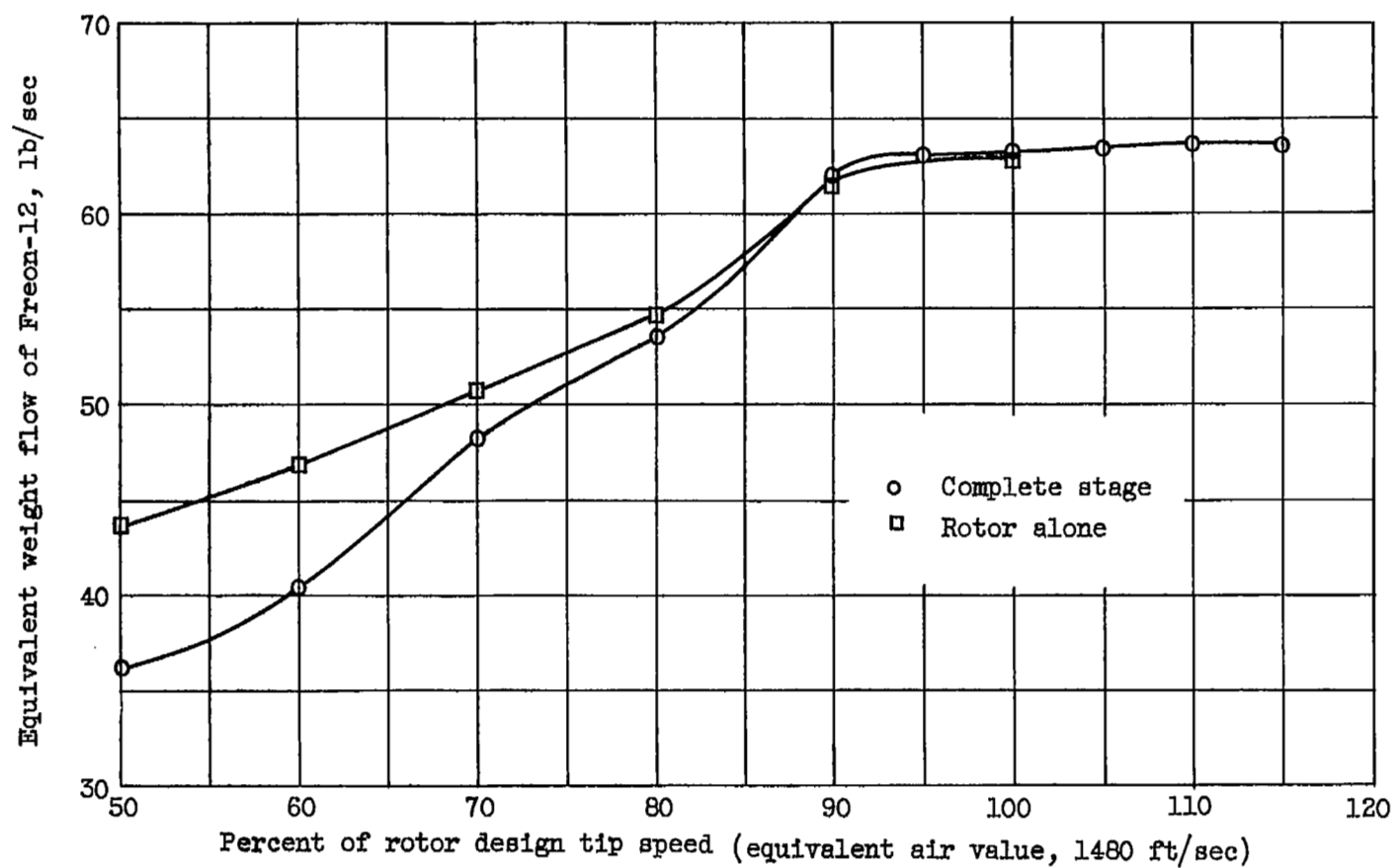
(b) Enthalpy rise.

Figure 6. - Concluded. Performance characteristics for 14-inch supersonic compressor.



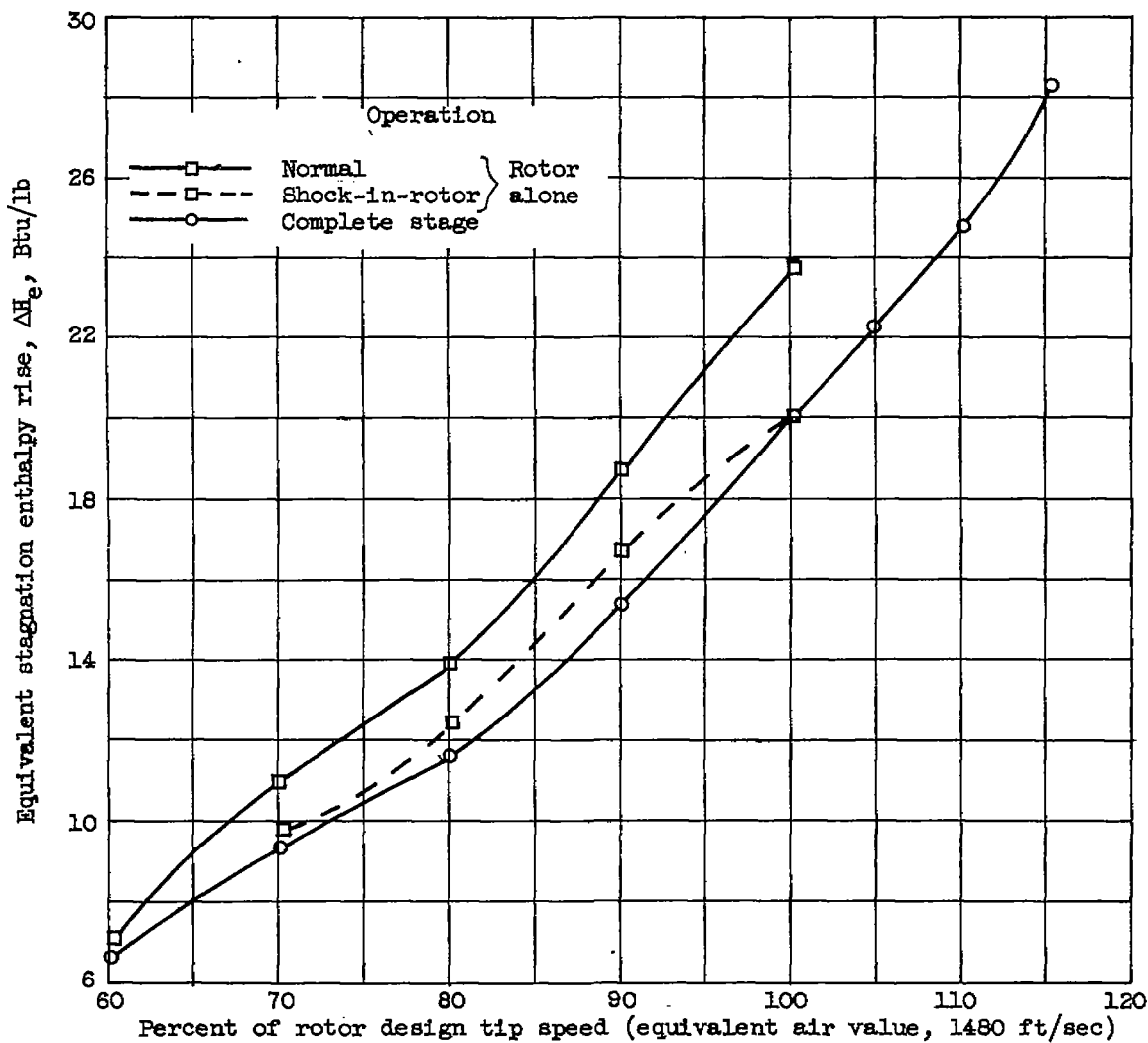
(a) Adiabatic efficiency.

Figure 7. - Comparison of performance of complete stage and rotor alone.



(b) Maximum weight flow.

Figure 7. - Continued. Comparison of performance of complete stage and rotor alone.



(c) Equivalent stagnation enthalpy rise.

Figure 7. - Concluded. Comparison of performance of complete stage and rotor alone.

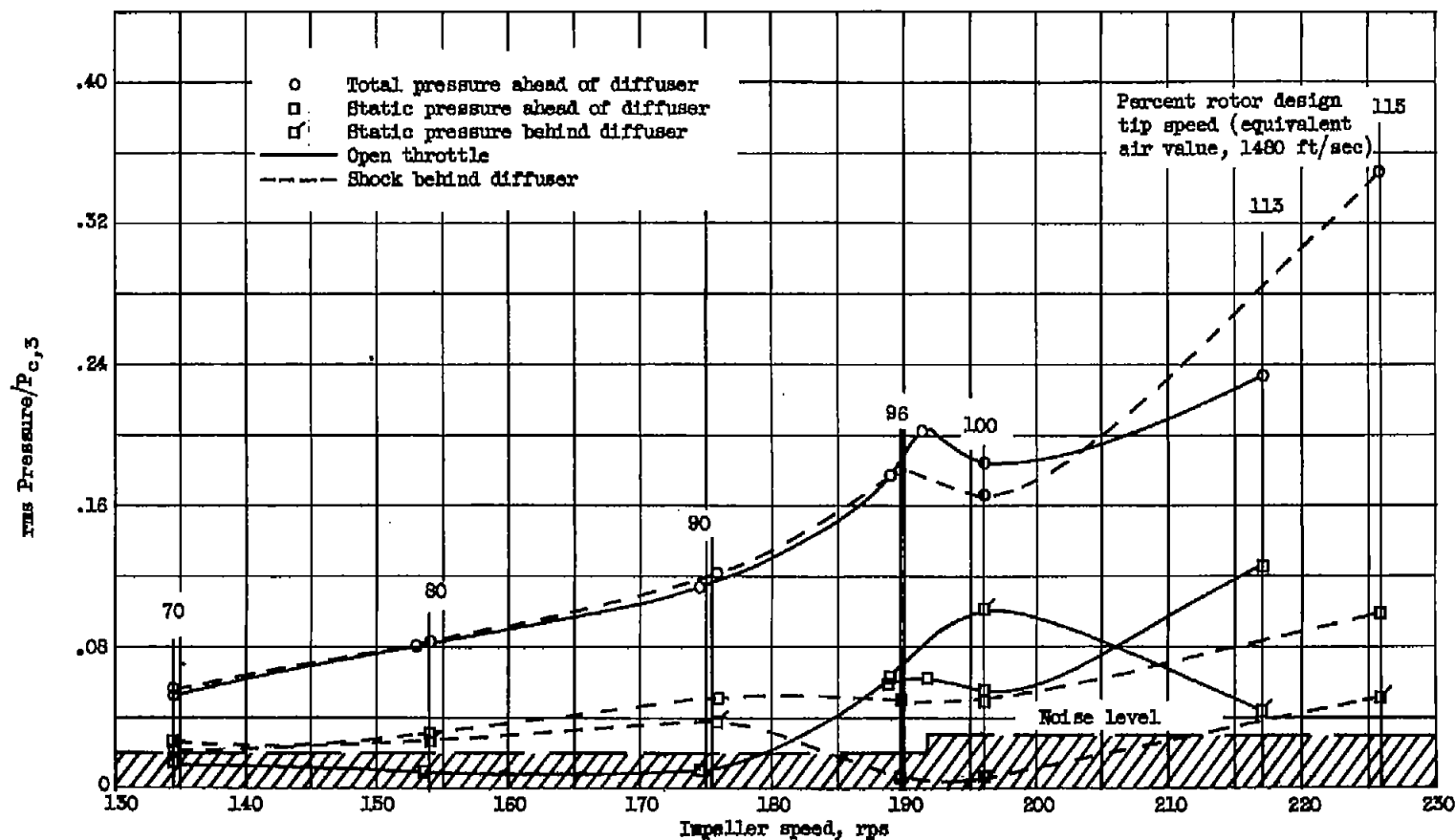


Figure 8. - Static- and total-pressure fluctuations for various speeds.

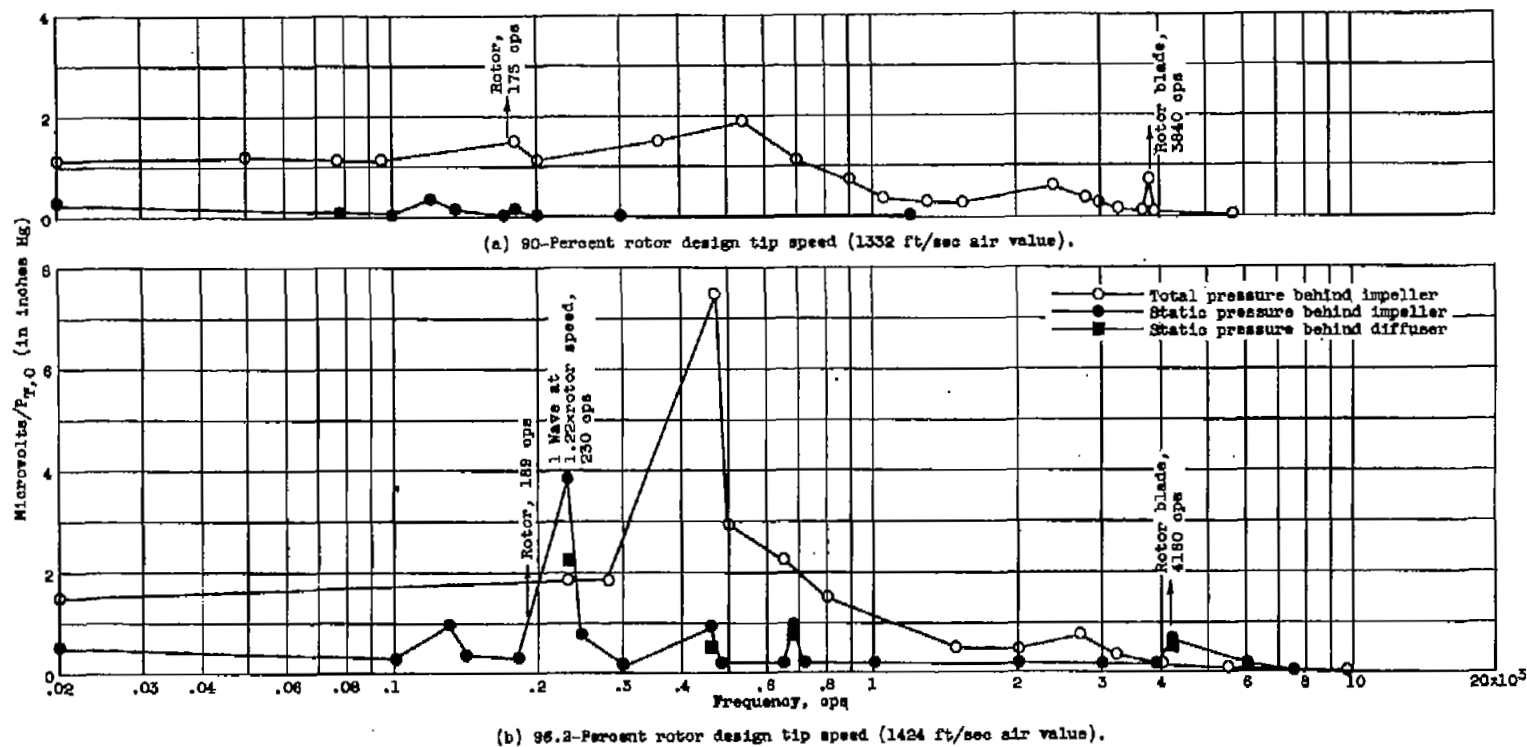
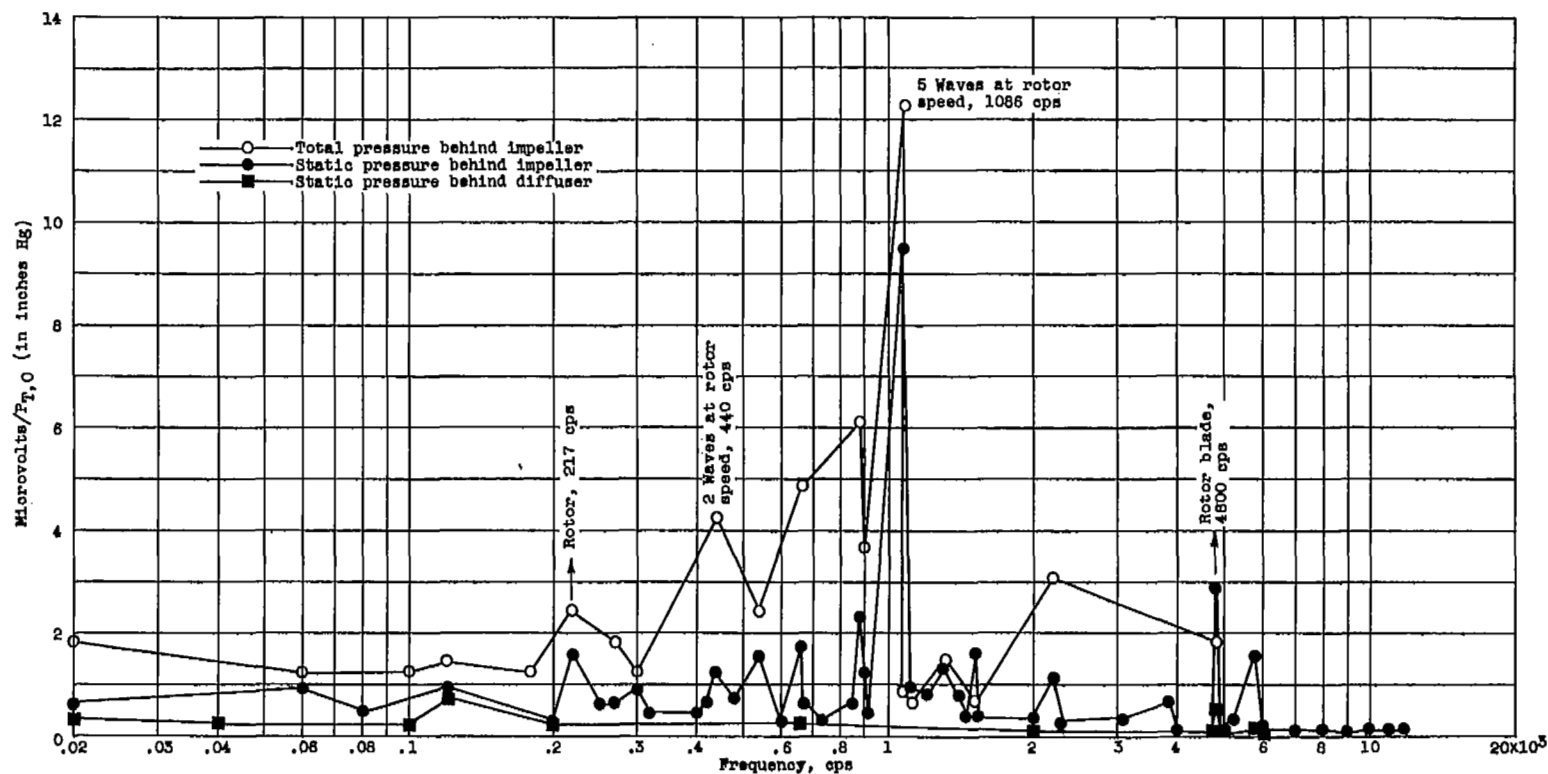
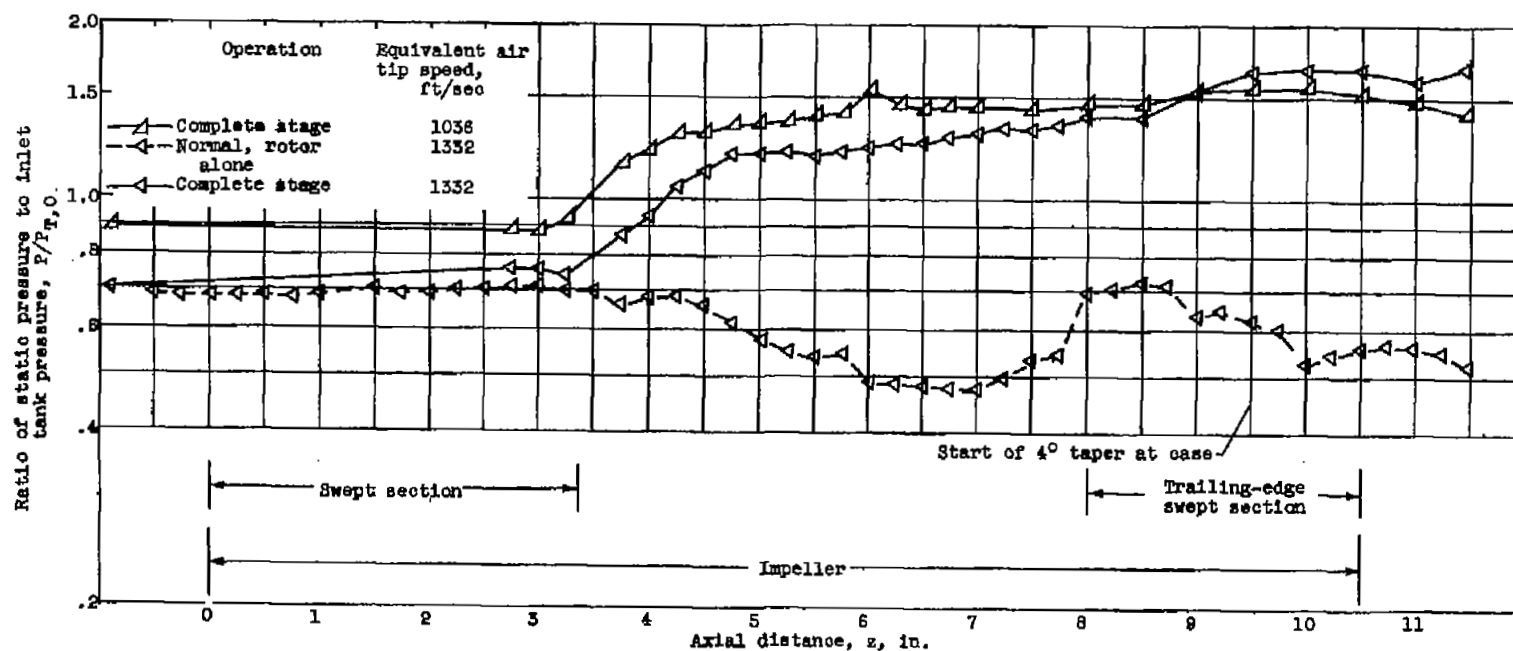


Figure 9. - Frequency distribution of intensity of fluctuation for various speeds.



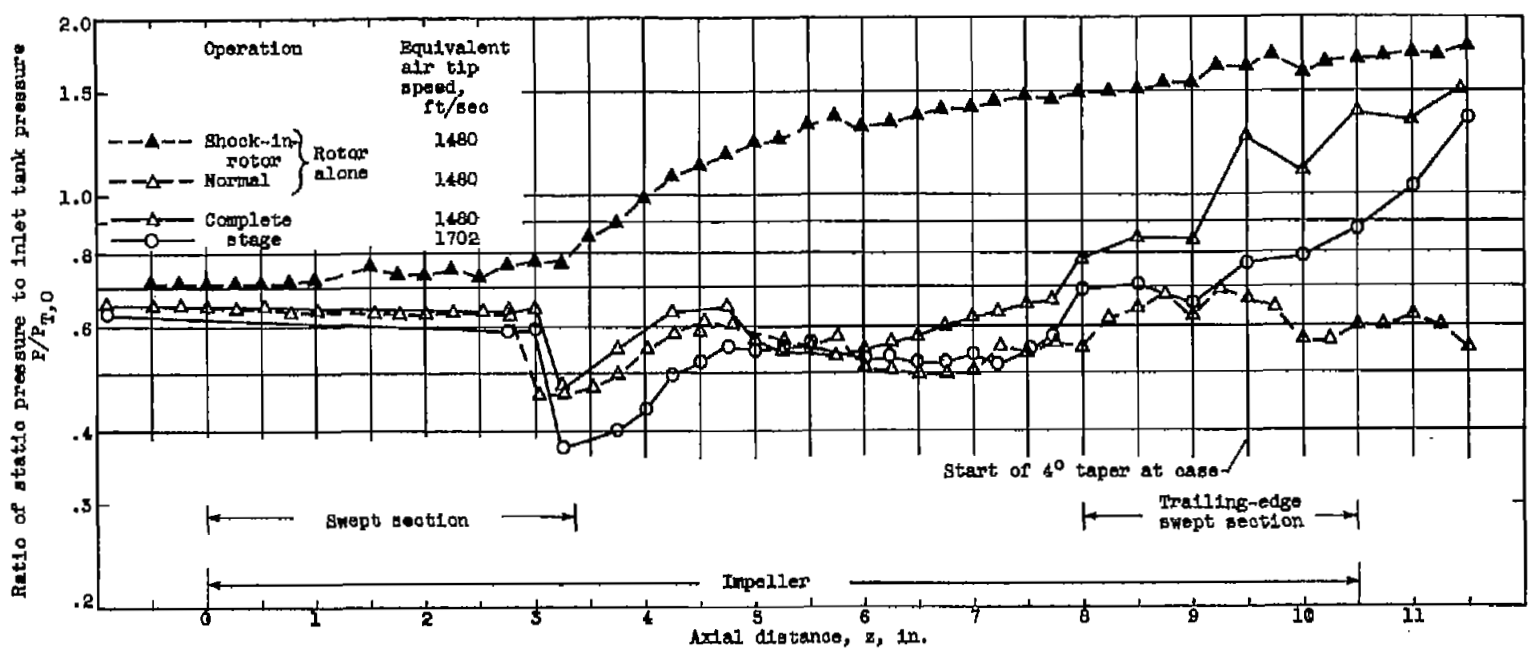
(c) 115-Percent rotor design tip speed (1672 ft/sec air value).

Figure 9. - Concluded. Frequency distribution of intensity of fluctuation for various speeds.



(a) Operation at equivalent air tip speeds of 1036 and 1332 feet per second.

Figure 10. - Impeller-case static-pressure distribution.



(b) Operation at equivalent air tip speeds of 1480 (design) and 1702 feet per second.

Figure 10. - Concluded. Impeller-casing static-pressure distribution.

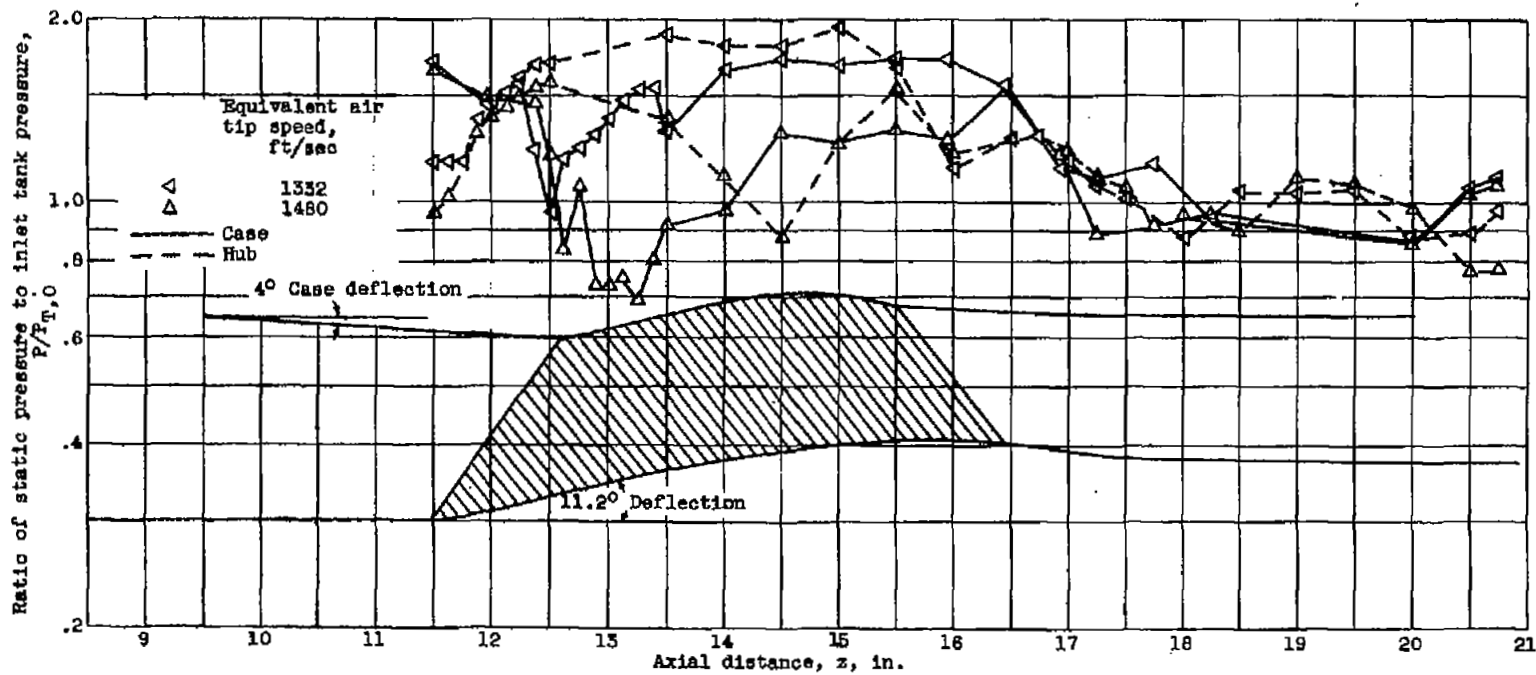


Figure 11. - Diffuser hub and case static-pressure distribution with open throttle for various speeds.

[REDACTED]

NASA Technical Library
3 1176 01435 7900

[REDACTED]

1
1

1
1

1
1

[REDACTED]